Chemical Science

ROYAL SOCIETY OF CHEMISTRY

EDGE ARTICLE

View Article Online
View Journal | View Issue

Check for updates

Cite this: *Chem. Sci.*, 2024, **15**, 14899

All publication charges for this article have been paid for by the Royal Society of Chemistry

Received 24th June 2024
Accepted 15th August 2024

DOI: 10.1039/d4sc04167d

rsc.li/chemical-science

Unexpected and divergent mechanosynthesis of furanoid-bridged fullerene dimers $C_{120}O$ and $C_{120}O_2$†

Gang Shao,‡[a] Yuan-Yuan Liu,‡[a] Chuang Niu,[b] Zheng-Chun Yin,[b] Shi-Qi Ye,[a] Yang-Rong Yao,[d] Muqing Chen,[e] Jun-Shen Chen,[a] Xu-Ling Xia,[a] Shangfeng Yang*[d] and Guan-Wu Wang*[abc]

An unexpected, divergent and efficient approach toward furanoid-bridged fullerene dimers $C_{120}O$ and $C_{120}O_2$ was established under different solvent-free ball-milling conditions by simply using pristine C_{60} as the starting material, water as the oxygen source and $FeCl_3$ as the mediator. The structures of $C_{120}O$ and $C_{120}O_2$ were unambiguously established by single-crystal X-ray crystallography. A plausible reaction mechanism is proposed on the basis of control experiments. Furthermore, $C_{120}O_2$ has been applied in organic solar cells as the third component and exhibits good performance.

Over the past three decades, [60]fullerene (C_{60}) and its derivatives have attracted significant attention due to their remarkable applications in numerous fields of materials science, biological applications and nanotechnology.[1] Fullerene dimers, including C_{120}, $C_{120}O$ and $C_{120}O_2$, are molecular structures linking two fullerene skeletons directly or *via* bridge(s) and are the fundamental subunits of fullerene polymers. Fullerene dimers exhibit many unique properties and thus have enormous potential for various applications.[2]

The selective formation of the dumbbell-shaped dimer C_{120} under solvent-free and mechanical milling conditions was first disclosed in 1997 by Wang *et al.*[3a] Since then, more solvent-free mechanochemical methods have been reported to generate fullerene dimer C_{120} *via* different promoters, such as inorganic salts, organic compounds and alkali metals.[3b,c] Later, the $FeCl_3$-mediated solution-phase synthesis of C_{120} was reported, providing a new approach for the synthesis of fullerene dimers (Scheme 1a).[4] To date, there are few methods for synthesizing furanoid-bridged dimers $C_{120}O$ and $C_{120}O_2$, and their syntheses are generally limited by the use of preprepared fullerene derivatives as the starting material, high temperatures, long reaction times and inert atmospheres.[5,6] $C_{120}O$ with one furan bridge was previously prepared by heating a mixture of $C_{60}O$ and 5–6 equiv. of C_{60} in the solid state at 200 °C for 1 h (19–20% yield)[5a] or in 1,2-dichlorobenzene (1,2-$C_6H_4Cl_2$) at 180 °C for 3 days (26% yield).[5b] $C_{120}O_2$ with cages bis-linked by adjacent furanoid bridges was formed in *ca.* 15% yield by heating solid $C_{120}O$ to 400 °C for 1 h in an argon atmosphere.[6] $C_{60}O$ was alternatively prepared by photooxygenation,[7a] oxidation with dimethyldioxirane,[7b] *m*-chloroperoxybenzoic acid,[7c] cytochrome P450 chemical models,[7d] methyltrioxorhenium–hydrogen peroxide[7e] or methyl (trifluoromethyl)dioxirane[7f] in yields ranging from 4% to 35%. Therefore, the overall yields of furanoid-bridged $C_{120}O$ and $C_{120}O_2$ starting from C_{60} are estimated to be only 0.8–9% and 0.1–1%, respectively. The identities of both $C_{120}O$ and $C_{120}O_2$ were deduced from their spectral data and theoretical calculations,[5,6,8] but confirmation by single-crystal X-ray structures is lacking. The harsh reaction conditions and use of preprepared $C_{60}O$ and $C_{120}O$ as the starting materials in these methodologies encounter obvious limitations and prevent their practical applications. Therefore, a more straightforward and efficient approach for accessing $C_{120}O$ and $C_{120}O_2$, particularly from pristine C_{60}, is highly desirable.

Mechanochemistry has gained increasing interest in recent years. Apart from making various chemical reactions possible under solvent-free conditions, mechanochemical reactions

---

[a] *Hefei National Research Center for Physical Sciences at Microscale and Department of Chemistry, University of Science and Technology of China, Hefei, Anhui 230026, P. R. China. E-mail: gwang@ustc.edu.cn*

[b] *Key Laboratory of Functional Molecular Solids, Ministry of Education, Anhui Laboratory of Molecule-Based Materials, and School of Chemistry and Materials Science, Anhui Normal University, Wuhu, Anhui 241002, P. R. China*

[c] *State Key Laboratory of Applied Organic Chemistry, Lanzhou University, Lanzhou, Gansu 730000, P. R. China*

[d] *Hefei National Research Center for Physical Sciences at the Microscale, CAS Key Laboratory of Materials for Energy Conversion, and Department of Materials Science and Engineering, University of Science and Technology of China, Hefei, Anhui, 230026, P. R. China. E-mail: sfyang@ustc.edu.cn*

[e] *School of Environment and Civil Engineering, Dongguan University of Technology, Dongguan, Guangdong, 523808, P. R. China*

† Electronic supplementary information (ESI) available: Detailed experimental procedures and characterization data, NMR spectra of $C_{120}O$ and $C_{120}O_2$, X-ray crystallographic data for $C_{120}O$ and $C_{120}O_2$. CCDC 2289163, 2289161. For ESI and crystallographic data in CIF or other electronic format see DOI: **https://doi.org/10.1039/d4sc04167d**

‡ Authors with equal contribution.

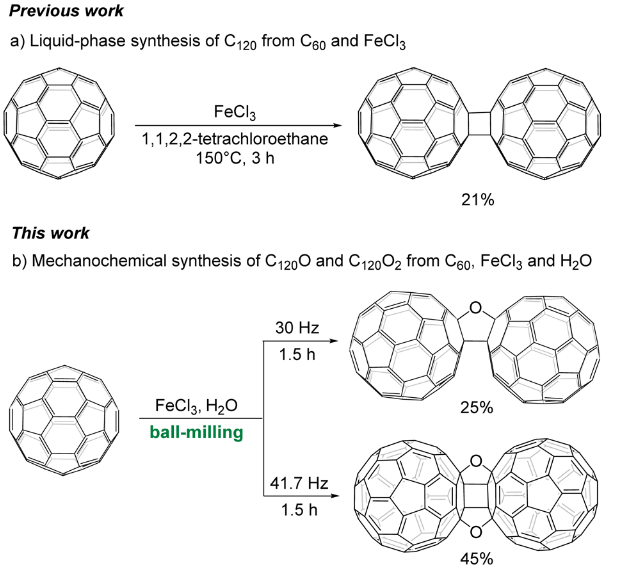

Scheme 1 Strategies for the synthesis of fullerene dimers.

feature many unique advantages, such as shorter reaction times, cleaner and safer reaction conditions, lower energy consumption, higher product yields and even different product selectivities.[9] C_{60} is barely soluble in common organic solvents, and its poor solubility somewhat restricts the exploration of its chemical reactions. Thus, mechanochemistry has emerged as an attractive alternative to conventional solution-based reactions in the field of fullerene chemistry.[10]

Due to the potential application of fullerene dimers and our continuous interest in fullerene mechanochemistry,[10,11] herein we disclose the unexpected, divergent and straightforward mechanosynthesis of furanoid-bridged fullerene dimers $C_{120}O$ and $C_{120}O_2$ directly from easily available pristine C_{60} (Scheme 1b). This highly efficient mechanochemical method will provide more possibilities for practical application of these fullerene dimers and new avenues for other bridged fullerene dimers.

In attempts to mechanochemically synthesize C_{120} from C_{60} and $FeCl_3$, it was intriguing to discover that the addition of H_2O could alter the reaction product from C_{120} to furanoid-bridged fullerene dimers. Therefore, the mechanochemical reaction of C_{60} with $FeCl_3$ and H_2O was systematically investigated. The results of the reaction optimizations for the furanoid-bridged dimer $C_{120}O$ are shown in Table 1. Initially, C_{60} (0.05 mmol), 6 equiv. of $FeCl_3$ and 15 equiv. of H_2O were added into a stainless steel jar (5 mL) together with 4 stainless steel balls (5 mm in diameter) under solvent-free and ambient conditions and milled vigorously at 1800 cycles per minute (30 Hz) in a GT 300 mixer mill at room temperature for 90 min. The reaction mixture was dissolved in 1,2-$C_6H_4Cl_2$ and monitored by high-performance liquid chromatography (HPLC) on a Cosmosil Buckyprep-D column with toluene as the mobile phase. It was found that the reaction mixture consisted of the furanoid-bridged dimer $C_{120}O$, dumbbell-shaped dimer C_{120} and unreacted C_{60}. The percentage of each component was calculated by quantitative analysis based on HPLC peak areas. The yield of $C_{120}O$ was thus determined to be 30%, in addition to the 33% yield of C_{120} (Table 1, entry 1). By increasing the amount of $FeCl_3$ to 7 equiv., the yield of $C_{120}O$ was enhanced to 33% (Table 1, entry 2), yet further increasing the amount of $FeCl_3$ to 8 equiv. resulted in a substantially decreased yield of 20% due to the formation of $C_{120}O_2$ (Table 1, entry 3). In addition, no benefit to the product yield could be achieved by shortening or prolonging the reaction time (Table 1, entries 4 and 5). When the reaction was attempted in the absence of H_2O, only trace amounts of C_{120} and $C_{120}O$ were detected, highlighting the pivotal role of H_2O in this mechanochemical reaction (Table 1, entry 6).

Table 1 Optimization of the reaction conditions to afford $C_{120}O^{a}$

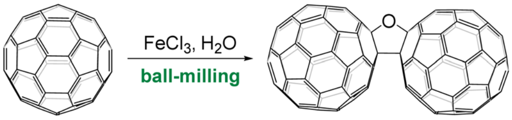

Entry	Ratio[b]	Yield of $C_{120}O$[c] (%)	Yield of C_{120}[c] (%)	Recovered C_{60}[c] (%)
1	1 : 6 : 15	30	33	37
2	**1 : 7 : 15**	**33**	**27**	**33**
3	1 : 8 : 15	20	11	28
4[d]	1 : 7 : 15	19	33	48
5[e]	1 : 7 : 15	29	16	32
6	1 : 7 : 0	Trace	Trace	36
7	1 : 7 : 20	28	34	34
8	1 : 7 : 10	30	26	43
9[f]	1 : 7 : 15	20	30	50
10[g]	1 : 7 : 15	26	38	29

[a] Unless otherwise noted, all reactions were performed with 0.05 mmol of C_{60}, $FeCl_3$, and H_2O together with 4 stainless steel balls (5 mm in diameter) in a stainless steel jar (5 mL) and milled vigorously (30 Hz) at room temperature for 90 min. [b] The molar ratio refers to $C_{60}/FeCl_3/H_2O$. [c] Based on HPLC area ratios on a Cosmosil Buckyprep-D (10 × 250 mm) column. [d] The reaction time was 60 min. [e] The reaction time was 120 min. [f] The reaction frequency was 25 Hz. [g] The reaction frequency was 35 Hz.

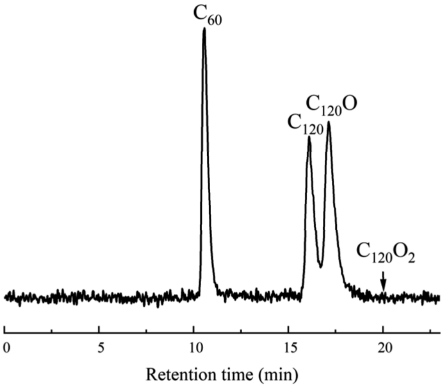

Fig. 1 HPLC chromatogram for the synthesis of $C_{120}O$ from C_{60}, H_2O and $FeCl_3$ under optimal ball-milling conditions.

Increasing or reducing the amount of H_2O resulted in a slightly lower yield (Table 1, entries 7 and 8 *vs.* entry 2). Furthermore, the product yield of $C_{120}O$ was lowered as the milling frequency was increased or decreased (Table 1, entries 9 and 10). On the basis of the results presented above and the isolated yield of $C_{120}O$ for each entry, the optimized conditions to afford $C_{120}O$ were determined as shown in entry 2 of Table 1: C_{60} (0.05 mmol), $FeCl_3$ (0.35 mmol), H_2O (0.75 mmol), a milling frequency of 30 Hz and a milling time of 90 min. The HPLC chromatogram on a Cosmosil Buckyprep-D (10 × 250 mm) column with toluene as the eluent at a flow rate of 1 mL min^{-1} and the detector wavelength at 326 nm is shown in Fig. 1. The retention times of C_{60}, C_{120}, $C_{120}O$ and $C_{120}O_2$ were 10.6 min, 16.1 min, 17.3 min and 20.0 min, respectively. The isolated yield of $C_{120}O$ by recycling HPLC on a Cosmosil Buckyprep-D (10 × 250 mm) column was 25%, which was significantly higher than the 0.8–9% for the two-step procedure starting from C_{60} (*vide supra*).

During the optimization process for the synthesis of the furanoid-bridged $C_{120}O$, it was found that increasing the amount of $FeCl_3$ as well as the milling frequency would favour the formation of the fullerene dimer $C_{120}O_2$ with bis-linked furanoid bridges. Therefore, we further modified our reaction conditions with the expectation of obtaining $C_{120}O_2$ dominantly or even selectively. The results from HPLC analyses are summarized in Table 2. A reaction mixture of C_{60} (0.05 mmol), 9 equiv. of $FeCl_3$ and 15 equiv. of H_2O was milled at 2500 cycles per minute (41.7 Hz) in a GT 600 mixer mill at room temperature for 90 min. To our delight, $C_{120}O_2$ was obtained in 57% yield along with a small amount of $C_{120}O$ (7%) and a trace amount of C_{120} (Table 2, entry 1). By increasing the amount of $FeCl_3$ to 10 equiv., the yield was enhanced to 69% (Table 2, entry

Table 2 Optimization of the reaction conditions to afford $C_{120}O_2$[a]

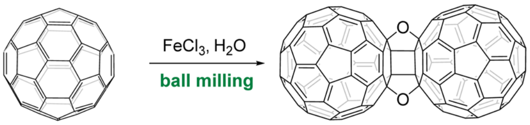

Entry	Additive	Ratio[b]	Yield of $C_{120}O_2$[c] (%)	Yield of $C_{120}O$[c] (%)	Yield of C_{120}[c] (%)	Recovered C_{60}[c] (%)
1	$FeCl_3$	1 : 9 : 15	57	7	Trace	36
2[c]	**$FeCl_3$**	**1 : 10 : 15**	**69**	**9**	**Trace**	**22**
3	$FeCl_3$	1 : 11 : 15	71	Trace	Trace	26
4	$FeCl_3$	1 : 12 : 15	80	0	0	20
5[d]	$FeCl_3$	1 : 10 : 15	52	10	Trace	32
6[e]	$FeCl_3$	1 : 10 : 15	67	7	Trace	26
7	$FeCl_3$	1 : 10 : 0	Trace	Trace	Trace	50
8	$FeCl_3$	1 : 10 : 10	57	7	Trace	36
9	$FeCl_3$	1 : 10 : 20	63	8	Trace	29
10[f]	$FeCl_3$	1 : 10 : 15	50	13	Trace	36
11[g]	$FeCl_3$	1 : 10 : 15	60	0	0	40
12	$AlCl_3$	1 : 10 : 15	0	Trace	50	50
13	$FeCl_2$	1 : 10 : 15	0	Trace	54	45
14	$NiCl_2$	1 : 10 : 15	0	Trace	44	55
15	Oxone	1 : 10 : 15	Trace	Trace	38	42
16	*m*-CPBA	1 : 10 : 15	Trace	Trace	41	45
17	H_2O_2	1 : 10 : 15	Trace	Trace	39	56
18[h]	$FeCl_3$	1 : 10 : 15	0	Trace	15	83
19[i]	$FeCl_3$	1 : 10 : 15	54	17	Trace	27
20[j]	$FeCl_3$	1 : 10 : 15	15	49	16	20

[a] Unless otherwise noted, all reactions were performed with 0.05 mmol of C_{60}, $FeCl_3$, and H_2O together with 4 stainless steel balls (5 mm in diameter) in a stainless steel jar (5 mL) and milled vigorously (41.7 Hz) at room temperature for 90 min. [b] The molar ratio refers to $C_{60}/FeCl_3/H_2O$. [c] Based on HPLC area ratios on a Cosmosil Buckyprep (4.6 × 250 mm) and/or Buckyprep-D (10 × 250 mm) column. [d] The reaction time was 60 min. [e] The reaction time was 120 min. [f] The reaction frequency was 35 Hz. [g] The reaction frequency was 45 Hz. [h] The reaction was performed in 1,1,2,2-tetrachloroethane (0.5 mL) at 150 °C for 48 h. [i] Under a N_2 atmosphere. [j] $C_{120}O$ was used instead of C_{60}.

2). Further increasing the amount of $FeCl_3$ could improve the selectivity and relative yield of $C_{120}O_2$ (Table 2, entries 3 and 4), but led to a decrease in the HPLC intensity, indicating that the amount of $C_{120}O_2$ was actually decreased and would lead to a lower isolated yield. It is believed that more insoluble oligomers were generated in the presence of more $FeCl_3$. Reducing the reaction time led to a lower yield, while increasing the reaction time had no beneficial effect (Table 2, entries 5 and 6). When this reaction was performed without H_2O, only a trace amount of $C_{120}O_2$ was observed, indicating that H_2O was crucial for promoting this reaction (Table 2, entry 7). In addition, no benefit to this reaction could be achieved by varying the amount of H_2O (Table 2, entries 8 and 9). Decreasing the milling frequency to 35 Hz resulted in more $C_{120}O$ and more recovered C_{60}, and increasing the milling frequency to 45 Hz did not improve the yield of $C_{120}O_2$ (Table 2, entries 10 and 11). In efforts to achieve more efficient synthesis of the peculiar $C_{120}O_2$, various Lewis acids, including $AlCl_3$, $FeCl_2$ and $NiCl_2$, and oxidizing agents, such as Oxone, *m*-chloroperbenzoic acid (*m*-CPBA) and H_2O_2, were explored. However, all of these additives were detrimental to the formation of $C_{120}O_2$ and afforded C_{120} exclusively (Table 2, entries 12–17). To compare the present solvent-free reaction with its liquid-phase counterpart, the reaction of C_{60} (0.05 mmol) with $FeCl_3$ (0.50 mmol) and H_2O (0.75 mmol) was performed in 0.5 mL of 1,1,2,2-tetrachloroethane at 150 °C for 48 h. Neither the desired product $C_{120}O_2$ nor $C_{120}O$ could be isolated, and C_{120} was instead formed in 15% yield (Table 2, entry 18). Other solvents, including toluene, chlorobenzene or 1,2-$C_6H_4Cl_2$, were also examined. However, the generation of $C_{120}O_2$ could not be observed in any of these solvents. Thus, it is obvious that the present mechanochemical solvent-free protocol shows advantages and uniqueness compared to the corresponding liquid-phase reaction. On the basis of the results presented above, the optimized conditions to afford the bisfuranoid-bridged dimer $C_{120}O_2$ were determined as shown in entry 2 of Table 2: C_{60} (0.05 mmol), $FeCl_3$ (0.50 mmol), H_2O (0.75 mmol), a milling frequency of 41.7 Hz and a milling time of 90 min. The HPLC chromatogram on a Cosmosil Buckyprep (4.6 × 250 mm) column with toluene as the eluent at a flow rate of 1 mL min^{-1} and the detector wavelength at 326 nm is shown in Fig. 2. The retention times of C_{60}, $C_{120}O$ and $C_{120}O_2$ were 7.5 min, 18.1 min and 20.7 min, respectively. The isolated yield of $C_{120}O_2$ by HPLC on a Cosmosil Buckyprep-D (10 × 250 mm) column was 45%, which was dramatically higher than the overall yield of 0.1–1% for the three-step process starting from C_{60} (*vide supra*).

The molecular structures of $C_{120}O$ and $C_{120}O_2$ were unambiguously established by single-crystal X-ray crystallography and are shown in Fig. 3. The single-crystal structure of $C_{120}O$ reveals that it has a furanoid ring linking two fullerene cages *via* [6,6]-ring junctions, clarifying the uncertainty of the oxygen connectivity to fullerenes.[12] The single-crystal structure of $C_{120}O_2$ shows that the two fullerene cages are connected by adjacent furanoid rings *via* [6,6]-ring junctions as in the case of $C_{120}O$, resulting in a central four-membered-ring bridge *via* [5,6]-ring junctions. The obtained single-crystal structure of our $C_{120}O_2$ confirms that it has C_{2v} symmetry, is the most stable and plausible structure predicted by theoretical calculations[8] and is neither the minor byproduct $C_{120}O_2$ with C_1 symmetry accompanying $C_{120}O$ from the solid–state reaction of C_{60} and $C_{60}O$ at 200 °C[13] nor the $C_{120}O_2$ isomer with C_2 symmetry from the dimerization of [5,6]-$C_{60}O$.[14] $C_{120}O$ and $C_{120}O_2$ were stable, and their thermogravimetric analyses (TGA) showed obvious weight loss above 370 °C (Fig. S5 and S6†).

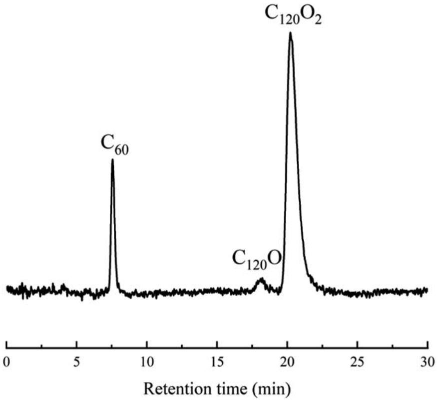

Fig. 2 HPLC chromatogram for the synthesis of $C_{120}O_2$ using $FeCl_3$ under optimal ball-milling conditions.

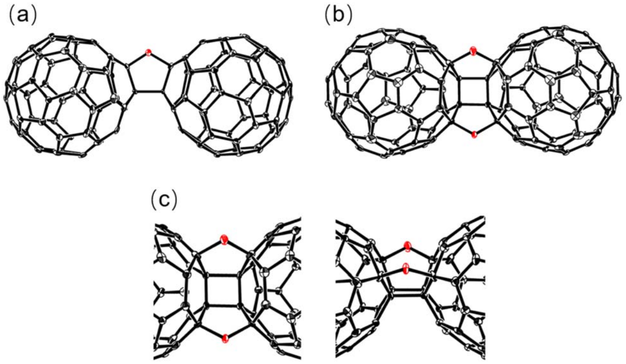

Fig. 3 ORTEP diagrams of (a) $C_{120}O$, (b) $C_{120}O_2$ and (c) top and side views around the two oxygen atoms in $C_{120}O_2$ with thermal ellipsoids shown at 10% probability. The solvent molecules were omitted for clarity.

To explore whether O_2 in the air atmosphere played a role during the milling process, the milling jar containing the reaction mixture was filled with nitrogen (N_2) in a glovebox and milled under the optimal conditions, which did not inhibit the production of $C_{120}O_2$ (Table 2, entry 19). When $C_{120}O$ was used to replace C_{60} under the optimal conditions, the yield of $C_{120}O_2$ decreased dramatically, and a considerable amount of C_{60} was produced (Table 2, entry 20). This result suggested that $C_{120}O_2$ was more likely to be generated directly from C_{60} rather than from $C_{120}O$ as a precursor. Therefore, $C_{120}O$ and $C_{120}O_2$ should be formed independently from C_{60} *via* different reaction pathways.

The mechanochemical $^{17}O/^{18}O$ labelling using $H_2{}^{17}O/H_2{}^{18}O$ has been reported.[15] To further identify the source of the bridging oxygen atom in $C_{120}O_2$, $H_2{}^{18}O$ was introduced to the reaction system, and the reaction process was monitored by HRMS. When $H_2{}^{18}O$ (10 atom % ^{18}O) was used, both $C_{120}{}^{16}O_2$

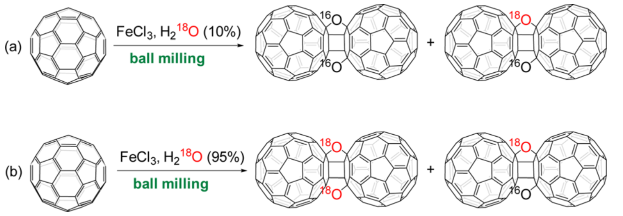

Scheme 2 ^{18}O labelling experiments with (a) $H_2{}^{18}O$ (10 atom % ^{18}O) and (b) $H_2{}^{18}O$ (95 atom % ^{18}O).

and $C_{120}{}^{16}O^{18}O$ were observed (Scheme 2a and Fig. S7†). Next, the addition of $H_2{}^{18}O$ (95 atom % ^{18}O) under the optimal reaction conditions provided $C_{120}{}^{16}O^{18}O$ and $C_{120}{}^{18}O_2$ (Scheme 2b and Fig. S8†). These results reinforced the conclusion that the bridging oxygen atom in $C_{120}O_2$ originated from H_2O. Furthermore, when potassium ferricyanide was added to the reaction mixture, a dark blue precipitate was generated (Fig. S9†), indicating the presence of ferrous ions. More importantly, the X-ray photoelectron spectroscopy (XPS) measurement of the reaction mixture revealed that an Fe(II) species was generated after the reaction was completed (Fig. S10†).

On the basis of the above experimental results and the literature,[16] a plausible reaction mechanism is outlined in Scheme 3. First, the initial coordination of C_{60} with $FeCl_3$ provides the complex $FeCl_2(\eta^2\text{-}C_{60})$ (**A**),[16] which is followed by the nucleophilic addition of H_2O to afford intermediate **B** in a 1,4-addition pattern. Loss of H^+ from intermediate **B** gives intermediate **C**. The hydroxy group in **C** directly attacks another molecule of pristine C_{60} to form an oxonium-bridged zwitterionic dimer **D**. Then, intramolecular cyclization with the removal of $FeCl_2$ and H^+ generates the furanoid-bridged dimer $C_{120}O$. With an increased amount of $FeCl_3$ and a higher milling frequency, the amount of the generated intermediate **C** can surpass that of the pristine C_{60}, and self-dimerization of **C** would dominate to give doubly oxonium-bridged intermediate **E**. Finally, **E** undergoes dual intramolecular cyclization with elimination of $FeCl_2$ and H^+ to provide the bisfuranoid-bridged dimer $C_{120}O_2$.

Given that fullerene derivatives have been applied in organic solar cells (OSCs) as the third component,[17] preliminary results showed that $C_{120}O_2$ could be employed in OSCs with the configuration of ITO/PEDOT:PSS/D18-Cl:N3:fullerene (1:1.4:0.12)/PDIN/Ag (Fig. 4). The device with $C_{120}O_2$ as the third component showed a PCE of 17.94% with a J_{SC} of 28.05 mA cm^{-2}, a V_{OC} of 0.86 V and an FF of 74.08%. The control device without a fullerene additive showed a lower PCE of 17.27% with a J_{SC} of 26.41 mA cm^{-2}, a V_{OC} of 0.87 V and an FF of 75.03%. The device with pristine C_{60} as the third component showed an inferior PCE of 15.77% with a J_{SC} of 26.68 mA cm^{-2}, a V_{OC} of 0.85 V and an FF of 69.24%. These results revealed that pristine C_{60} had an adverse effect, while the bisfuranoid-bridged dimer $C_{120}O_2$ was a promising third-component material in the active layer of the OSCs. Unfortunately, the synthesized $C_{120}O$ has limited solubility and could not be used as a third component in the current OSCs.

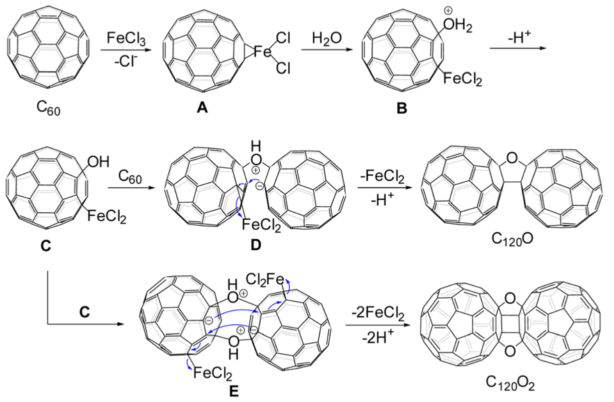

Scheme 3 Proposed reaction mechanism.

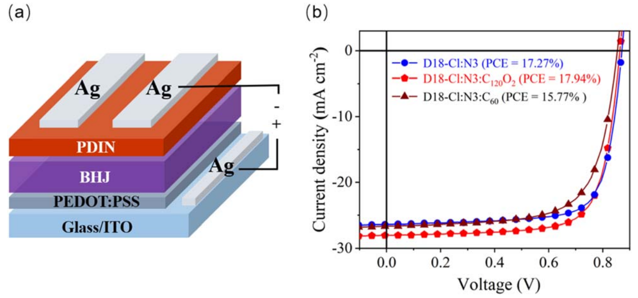

Fig. 4 (a) Schematic illustration of the OSC structure used in this work. (b) *J*–*V* curves of D18-Cl:N3 (blue line), D18-Cl:N3:$C_{120}O_2$ (red line) and D18-Cl:N3:C_{60} (brown line)-based OSCs.

Conclusions

In summary, we have disclosed the unexpected, divergent and highly efficient synthesis of furanoid-linked $C_{120}O$ and $C_{120}O_2$ from the $FeCl_3$-mediated mechanochemical reaction of C_{60} with H_2O as the bridging oxygen source at room temperature under an air atmosphere. The present protocol avoids the usage of preprepared $C_{60}O$ and $C_{120}O$. The selective synthesis of $C_{120}O$ with one furanoid bridge and $C_{120}O_2$ with two furanoid bridges directly from pristine C_{60} can be achieved by altering the amount of $FeCl_3$ and the milling frequency. The excellent yields, simplicity of this synthetic process and solvent-free and ambient conditions compared to those of previous multistep processes make this mechanochemical protocol an efficient method for the divergent synthesis of $C_{120}O$ and $C_{120}O_2$. The specific structures of $C_{120}O$ and $C_{120}O_2$ have been unequivocally established by single-crystal X-ray crystallography. A plausible reaction mechanism has been proposed based on the control experiments. The bisfuranoid-bridged dimer $C_{120}O_2$ has also been utilized as the third component in organic solar cells and has shown improved performance in OSC devices.

Data availability

The data supporting the findings of this study are available within the article and its ESI.†

Author contributions

G.-W. W. and S. Y. supervised the project. G. S. and J.-S. C. performed experiments and data analysis and wrote original manuscript, Y.-Y. L. fabricated the organic solar cell devices and analyzed data. G. S., C. N., Z.-C. Y., Y.-R. Y. and M. C. characterized the X-ray structures. S.-Q. Y. performed XPS test and data analysis. X.-L. X. assisted in data analysis and original manuscript preparation. G.-W. W. acquired funding and wrote the manuscript. All the authors contributed with comments and revisions to the manuscript and gave approval to the final version.

Conflicts of interest

There are no conflicts to declare.

Acknowledgements

We are grateful for financial support from the National Natural Science Foundation of China (22071231, 21372211).

Notes and references

1 For reviews, see: (*a*) A. L. Balch and K. Winkler, *Chem. Rev.*, 2016, **116**, 3812–3882; (*b*) M. Chen, R. Guan and S. Yang, *Adv. Sci.*, 2019, **6**, 1800941; (*c*) K. Harano and E. Nakamura, *Acc. Chem. Res.*, 2019, **52**, 2090–2100; (*d*) T. Umeyama and H. Imahori, *Acc. Chem. Res.*, 2019, **52**, 2046–2055; (*e*) L. Jia, M. Chen and S. Yang, *Mater. Chem. Front.*, 2020, **4**, 2256–2282; (*f*) Z. Xing, S.-H. Li and S. Yang, *Small Struct.*, 2022, **3**, 2200012.

2 J. L. Segura and N. Martín, *Chem. Soc. Rev.*, 2000, **29**, 13–25.

3 (*a*) G.-W. Wang, K. Komatsu, Y. Murata and M. Shiro, *Nature*, 1997, **387**, 583–586; (*b*) K. Komatsu, G.-W. Wang, Y. Murata, T. Tanaka, K. Fujiwara, K. Yamamoto and M. Saunders, *J. Org. Chem.*, 1998, **63**, 9358–9366; (*c*) K. Komatsu, K. Fujiwara, T. Tanaka and Y. Murata, *Carbon*, 2000, **38**, 1529–1534.

4 M. Hashiguchi, H. Inada and Y. Matsuo, *Carbon*, 2013, **61**, 418–422.

5 (*a*) S. Lebedkin, S. Ballenweg, J. Gross, R. Taylor and W. Krätschmer, *Tetrahedron Lett.*, 1995, **36**, 4971–4974; (*b*) A. B. Smith III, H. Tokuyama, R. M. Strongin, G. T. Furst, W. J. Romanow, B. T. Chait, U. A. Mirza and I. Haller, *J. Am. Chem. Soc.*, 1995, **117**, 9359–9360.

6 A. Gromov, S. Lebedkin, S. Ballenweg, A. G. Avent, R. Taylor and W. Krätschmer, *Chem. Commun.*, 1997, 209–210.

7 (*a*) K. M. Creegan, J. L. Robbins, W. K. Robbins, J. M. Millar, R. D. Sherwood, P. J. Tindall, D. M. Cox, A. B. Smith, III, J. P. McCauley, Jr, D. R. Jones and R. T. Gallagher, *J. Am. Chem. Soc.*, 1992, **114**, 1103–1105; (*b*) Y. Elemes, S. K. Silverman, C. Sheu, M. Kao, C. S. Foote, M. M. Alvarez and R. L. Whetten, *Angew. Chem., Int. Ed. Engl.*, 1992, **31**, 351–353; (*c*) A. L. Balch, D. A. Costa, B. C. Noll and M. M. Olmstead, *J. Am. Chem. Soc.*, 1995, **117**, 8926–8932; (*d*) T. Hamano, T. Mashino and M. Hirobe, *J. Chem. Soc., Chem. Commun.*, 1995, 1537–1538; (*e*) R. W. Murray and K. Iyanar, *Tetrahedron Lett.*, 1997, **38**, 335–338; (*f*) C. Fusco, R. Seraglia, R. Curci and V. Lucchini, *J. Org. Chem.*, 1999, **64**, 8363–8368.

8 P. W. Fowler, D. Mitchell, R. Taylor and G. Seifert, *J. Chem. Soc., Perkin Trans. 2*, 1997, 1901–1905.

9 For reviews, see: (*a*) G.-W. Wang, *Chem. Soc. Rev.*, 2013, **42**, 7668–7700; (*b*) J. G. Hernández and C. Bolm, *J. Org. Chem.*, 2017, **82**, 4007–4019; (*c*) M. Leonardi, M. Villacampa and J. C. Menéndez, *Chem. Sci.*, 2018, **9**, 2042–2064; (*d*) J. Andersen and J. Mack, *Green Chem.*, 2018, **20**, 1435–1443; (*e*) T. Friščić, C. Mottillo and H. M. Titi, *Angew. Chem., Int. Ed.*, 2020, **59**, 1018–1029; (*f*) K. J. Ardila-Fierro and J. G. Hernández, *Angew. Chem., Int. Ed.*, 2024, **63**, e202317638.

10 For reviews, see: (*a*) S. -E Zhu, F. Li and G.-W. Wang, *Chem. Soc. Rev.*, 2013, **42**, 7535–7570; (*b*) G.-W. Wang, *Chin. J. Chem.*, 2021, **39**, 1797–1803.

11 For recent examples, see: (*a*) H.-W. Liu, H. Xu, G. Shao and G.-W. Wang, *Org. Lett.*, 2019, **21**, 2625–2628; (*b*) G. Shao, C. Niu, H.-W. Liu, H. Yang, J.-S. Chen, Y.-R. Yao, S. Yang and G.-W. Wang, *Org. Lett.*, 2023, **25**, 1229–1234.

12 M. M. Olmstead, D. A. Costa, K. Maitra, B. C. Noll, S. L. Phillips, P. M. Van Calcar and A. L. Balch, *J. Am. Chem. Soc.*, 1999, **121**, 7090–7097.

13 A. Gromov, S. Lebedkin, W. E. Hull and W. Krätschmer, *J. Phys. Chem. A*, 1998, **102**, 4997–5005.

14 D. Tsyboulski, D. Heymann, S. M. Bachilo, L. B. Alemany and R. B. Weisman, *J. Am. Chem. Soc.*, 2004, **126**, 7350–7358.

15 J. Špačková, C. Fabra, G. Cazals, M. Hubert-Roux, I. Schmitz-Afonso, I. Goldberga, D. Berthomieu, A. Lebrun, T.-X. Métro and D. Laurencin, *Chem. Commun.*, 2021, **51**, 6812–6815.

16 (*a*) N. Malic, P. J. Nichols, M. Makha and C. L. Raston, *Cryst. Growth Des.*, 2009, **9**, 863–866; (*b*) D. V. Konarev, S. S. Khasanov, M. A. Faraonov and R. N. Lyubovskaya, *CrystEngComm*, 2012, **14**, 4350–4356; (*c*) D. A. Garcia-hernandez, F. Cataldo and A. Manchado, *Fullerenes, Nanotub. Carbon Nanostruct.*, 2016, **24**, 225–233; (*d*) M. A. Faraonov, A. V. Kuzmin, S. S. Khasanov, A. F. Shestakov, A. Otsuka, H. Yamochi, H. Kitagawa and D. V. Konarev, *Inorg. Chem.*, 2022, **61**, 20144–20149.

17 For examples, see: (*a*) R. Yu, H. Yao, Y. Cui, L. Hong, C. He and J. Hou, *Adv. Mater.*, 2019, **31**, 1902302; (*b*) M.-A. Pan, T.-K. Lau, Y. Tang, Y.-C. Wu, T. Liu, K. Li, M.-C. Chen, X. Lu, W. Ma and C. Zhan, *J. Mater. Chem. A*, 2019, **7**, 20713–20722; (*c*) B. Qiu, S. Chen, C. Sun, J. Yuan, X. Zhang, C. Zhu, S. Qin, L. Meng, Y. Zhang, C. Yang, Y. Zou and Y. Li, *Sol. RRL*, 2020, **4**, 1900540; (*d*) D. Hu, H. Tang, J. Lv, Z. Liao, Q. Chen, H. Chen and S. Lu, *Sustain. Energy Fuels*, 2021, **5**, 3593–3597; (*e*) Z. Liu and H.-E. Wang, *Sol. Energy*, 2021, **230**, 549–557; (*f*) Z.-C. Yin, M. Li, C. Niu, W.-F. Wang, W.-R. Liu, Q.-W. Zhang and G.-W. Wang, *Angew. Chem., Int. Ed.*, 2023, **62**, e202304321; (*g*) T.-X. Liu, X. Wang, S. Xia, M. Chen, M. Li, P. Yang, N. Ma, Z. Hu, S. Yang, G. Zhang and G.-W. Wang, *Angew. Chem., Int. Ed.*, 2023, **62**, e202313074.